Continental Shelf Research 28 (2008) 1231–1245

Contents lists available at ScienceDirect

Continental Shelf Research

journal homepage: www.elsevier.com/locate/csr

Northeast storms ranked by wind stress and wave-generated bottom stress observed in Massachusetts Bay, 1990–2006

Bradford Butman[a,*], Christopher R. Sherwood[a], P. Soupy Dalyander[b,1]

[a] US Geological Survey, 384 Woods Hole Road, Woods Hole, MA 02543, USA
[b] Integrated Statistics, Inc., 16 Sumner Street, Woods Hole, MA 02543, USA

ARTICLE INFO

Article history:
Received 16 August 2007
Received in revised form
11 February 2008
Accepted 13 February 2008
Available online 4 March 2008

Keywords:
Storms
Northeasters
Climatology
Bottom stress
Wind stress
Surface water waves
USA
Gulf of Maine
Massachusetts Bay

ABSTRACT

Along the coast of the northeastern United States, strong winds blowing from the northeast are often associated with storms called northeasters, coastal storms that strongly influence weather. In addition to effects caused by wind stress, the sea floor is affected by bottom stress associated with these storms. Bottom stress caused by orbital velocities associated with surface waves integrated over the duration of a storm is a metric of storm strength at the sea floor. Near-bottom wave-orbital velocities calculated by using measurements of significant wave height and dominant wave period and the parametric spectral method described in Wiberg and Sherwood [Wiberg, P.L., Sherwood, C.R. Calculating wave-generated bottom orbital velocities from surface wave parameters. Computers in Geosciences, in press] compared well with observations in Massachusetts Bay. Integrated bottom-wave stress (called IWAVES), calculated at 30 m water depth, and a companion storm-strength metric, integrated surface wind stress at 10 m (called IWINDS), are used to provide an overview of the strength, frequency, and timing of large storms in Massachusetts Bay over a 17-year period from January 1990 through December 2006. These new metrics reflect both storm duration and intensity. Northeast storms were the major cause of large waves in Massachusetts Bay because of the long fetch to the east: of the strongest 10% of storms ($n = 38$) ranked by IWAVES, 22 had vector-averaged wind stress from the northeast quadrant. The Blizzard of December 1992, the Perfect Storm of October 1991, and a December 2003 storm were the strongest three storms ranked by IWAVES and IWINDS, and all were northeasters. IWAVES integrated over the winter season (defined as October–May) ranged by about a factor of 11; the winters with the highest integrated IWAVES were 1992–1993 and 2004–2005 and the winter with the lowest integrated IWAVES was 2001–2002. May 2005 was the only month in the 17-year record that two of the nine strongest northeast storms ranked by IWINDS occurred in the same month or year; these were also the only storms of the nine strongest northeast storms to occur in the spring.

1. Introduction

Along the coast of the northeastern United States, strong winds blowing from the northeast are often associated with storms called "northeasters," coastal storms that strongly influence weather. These extratropical cyclones typically form off the mid-Atlantic coast and move northeastward as they strengthen. The strength and duration of winds and the surface waves associated with these storms at a particular location depend on the storm's central pressure, size, path, and speed of travel. Classification schemes and rankings for northeasters and meteorological events have been described by Dolan and Davis (1992), Zielinski (2002), and Hart and Grumm (2001). The long-term variability (Zhang et al., 2000) and characteristics of particular storms have also been investigated (see references cited in Hart and Grumm, 2001).

In addition to effects caused by the surface wind stress, which typically receive much attention, northeasters affect the sea floor. For example, observations in Massachusetts Bay and elsewhere show that the bottom stress associated with storms is a dominant cause of resuspension of bottom sediments. This paper introduces bottom stress caused by surface waves and integrated over the duration of a storm as a metric for the strength of storms at the sea floor. The paper provides motivation for use of this new storm metric and presents a companion storm metric based on integrated wind stress. The methods outlined by Wiberg and Sherwood (in press) for calculating near-bottom wave-orbital velocities and bottom-wave stress using surface-wave observations were tested using data obtained in Massachusetts Bay.

* Corresponding author. Tel.: +1 508 457 2212.
E-mail addresses: bbutman@usgs.gov (B. Butman), csherwood@usgs.gov (C.R. Sherwood), sdalyander@usgs.gov (P.S. Dalyander).

[1] Previously published as P. Soupy Alexander.

0278-4343/$ - see front matter © 2008 Elsevier Ltd. All rights reserved.
doi:10.1016/j.csr.2008.02.010

The surface- and bottom-stress storm metrics are used to provide an overview of the strength, frequency, and timing of large storms, particularly northeasters, in Massachusetts Bay based on wind and wave observations from January 1990 through December 2006.

2. Effects of northeasters

This investigation of the strength of northeasters was motivated by observations of their effects in Massachusetts Bay, a semi-enclosed embayment in the western Gulf of Maine about 50 km wide and 100 km long (Fig. 1). Long-term near-bottom observations at 30 m water depth show that bottom stress caused by surface waves is the principal cause of sediment resuspension (Butman et al., 2004, 2007), and that the largest waves are associated with northeasters because Massachusetts Bay is surrounded by land except to the east. Modeling studies of sediment transport caused by northeasters (Butman et al., 2007; Warner et al., 2008) used the ranking strategy presented here to identify the largest storms and their characteristics. These studies show that a sequence of northeast storms, modeled after the strongest to occur between 1990 and 2006, can rework a spatially uniform mixture of sediments to produce a surficial sediment distribution that is similar to the present day. They also showed that northeast storms transport sediments from Boston Harbor to the long-term depositional areas of Stellwagen Basin and Cape Cod Bay.

A second motivation for this storm ranking investigation was to place two northeast storm events in historical context. Long-term observations of the surficial sediments were made at site 3 (Fig. 1) in western Massachusetts Bay as part of a long-term USGS—Massachusetts Water Resources Authority Program to monitor the potential effects of the new ocean outfall (Bothner and Butman, 2007). The concentrations of silver, clay, and *Clostridium perfringens* spores at this site increased by a factor of two or more following the northeaster "Blizzard of December 1992"; these were the largest changes in surficial (upper 2 cm) sediment properties observed in the 17-year time-series, and they are attributed to the deposition of fine-grained contaminated sediment transported to this site during the northeaster (Bothner et al., 2007). The second event was an extensive bloom of the toxic dinoflagellate *Alexandrium fundyense* in the western Gulf of Maine in the spring of 2005, the largest bloom since 1972 (Anderson

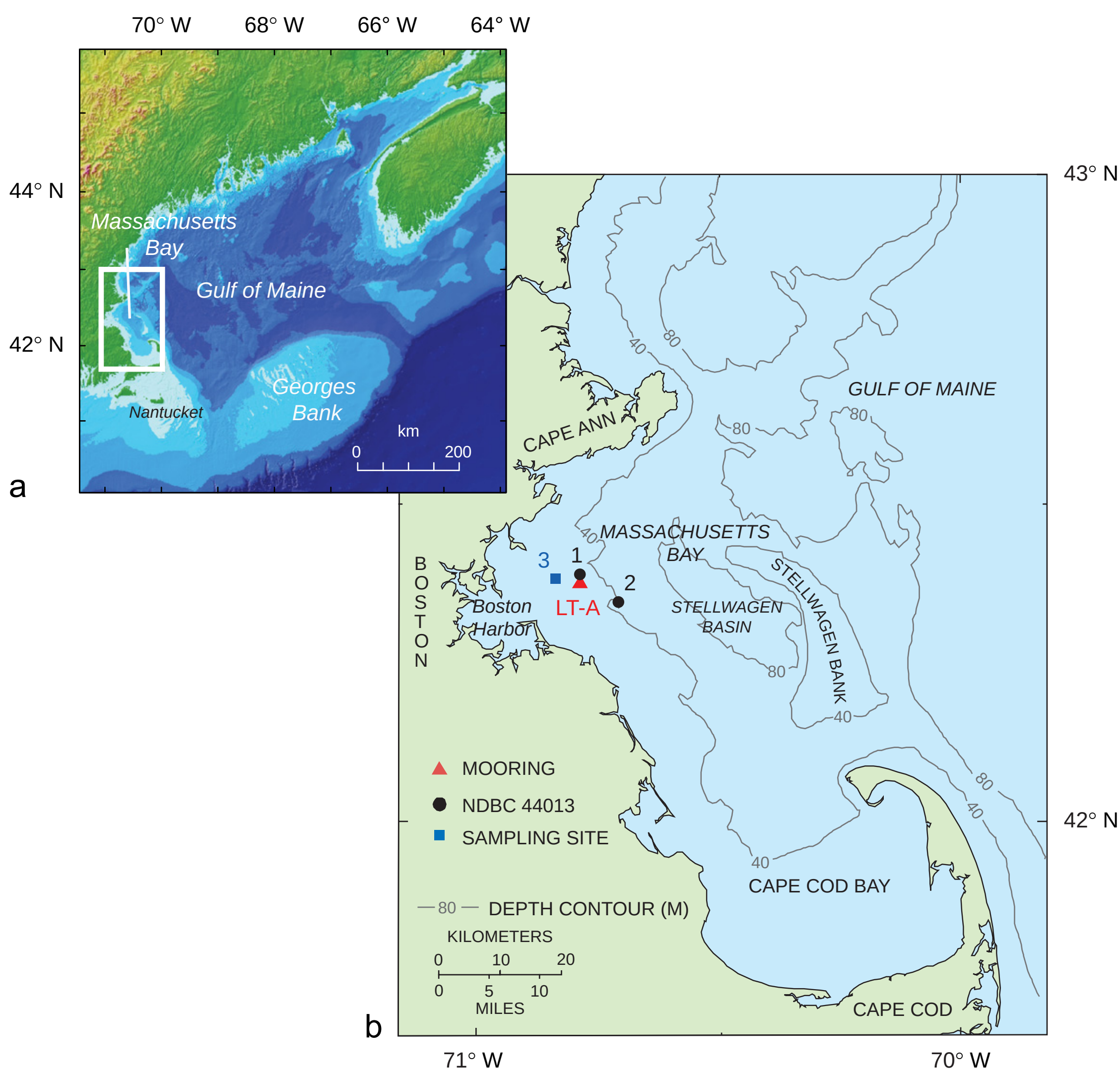

Fig. 1. (a) Map showing the location of Massachusetts Bay in the western Gulf of Maine (image from Roworth and Signell (1998)). (b) Map showing Massachusetts Bay. Wind and wave measurements were made at NDBC Station 44013 at site 1 (approximately 30 m water depth) from a 10 m Large Navigational Buoy from 1990 to 1993 and at site 2 (approximately 55 m water depth) from a 3 m discus buoy from 1993 to 2006. Bottom current observations were made at LT-A (32 m water depth). Long-term observations of sediment texture and contaminant concentrations were made at site 3 (Bothner et al., 2007). Contours show water depth in meters.

et al., 2005b). Currents driven by two northeasters in May 2005 transported this bloom along the coast of the western Gulf of Maine, into Massachusetts Bay, and to the south of Nantucket Island. For both of these events, it was of interest to determine the characteristics of the northeasters and how often storms of similar magnitude occurred.

These observations illustrate two ways that northeasters affect Massachusetts Bay and the western Gulf of Maine. First, large long-period waves are generated by northeast winds, and the oscillatory bottom currents associated with these waves cause significant bottom stress. Depending on the wave height, period, and water depth, the bottom-wave stress may resuspend sediments in water depths as much as 80 m (Butman et al., 2007). Second, northeast winds drive a coastal current southwestward along the Maine coast. These winds are also downwelling-favorable; fresh water from coastal river discharge and materials associated with it are trapped against the coast and move southwestward in the coastal current (Anderson et al., 2005a).

3. Data and stress calculations

Wind observations made at the National Oceanic and Atmospheric Administration (NOAA) National Data Buoy Center (NDBC) Station 44013 in Massachusetts Bay (sites 1 and 2, Fig. 1) were obtained for a 17-year period from January 1990 through December 2006 (NOAA NDBC). Between October 1990 and October 1993, the anemometer was on a Large Navigational Buoy (LNB; a 10 m discus buoy) at 42°22.80′N, 70°46.80′W (where the water depth was approximately 30 m) at a height of 13.8 m. Between November 1993 and July 1997, the anemometer was on a 3 m discus buoy at 42°21.05′N, 70°41.48′W (where the water depth was approximately 55 m) at a height of 5 m. From November 1997 to 2006, the 3 m buoy was at 42°21.23′N, 70°41.48′W. All wind-speed observations were adjusted to a 10 m height and wind stress was computed from wind speed by the method of Large and Pond (1981) assuming neutral stability of the atmosphere. The wind record has five gaps (from 09/01/1990 to 10/04/1990, 06/18/1994 to 09/20/1994, 04/01/1996 to 04/22/1996, 07/07/1997 to 11/11/1997, and from 01/01/2001 to 03/31/2001). No attempt was made to fill these gaps.

Surface-wave observations made at NDBC 44013 were also obtained for the period 1990–2006. For the period 1990–1996, summary statistics of significant wave height (H_s), dominant (or peak) wave period (T_p), and average wave period (T_{av}) were available. For the period 1996–2006, a full wave spectrum was available in addition to the summary statistics. There is one gap in the wave record from 07/07/1997 to 11/11/1997.

Representative near-bottom wave-orbital velocities (u_{br}) caused by surface waves were computed at selected depths from the wave observations using a parametric spectral method described by Wiberg and Sherwood (in press) and assuming the Donelan spectra. This parametric method uses an assumed wave-spectrum shape defined by H_s and T_p and calculates u_{br}, the amplitude of a monochromatic wave with the same variance as the full spectrum. For the period 1997–2006, for which the full surface-wave spectra are available, the wave-orbital speeds calculated from the full spectrum and those calculated by the parametric method assuming the Donelan spectra typically agree within a few percent (Fig. 2a). Wave-orbital velocities calculated by the parametric method also agree well with wave-orbital velocities measured from a bottom tripod system adjacent to NDBC 44013 during periods in 1993 (record 374) and 1996 (record 413) (Fig. 2b). We conclude that the parametric spectral method of Wiberg and Sherwood (in press) provides a consistent way to calculate near-bottom wave-orbital velocities and associated periods (T_b) from the summary H_s and T_p measurements over the 17-year period of observations.

Wave bottom stress (τ_{bw}) was calculated from near-bottom wave-orbital velocity (u_{br}) and period by using the wave-current bottom boundary layer model of Madsen (1994). A physical roughness of 0.00167 m (approximately equivalent to a grain roughness (2.5 times the grain diameter) for coarse sand) was used. Because continuous near-bottom current measurements are not available, the Madsen (1994) formulation collapsed to a wave-friction calculation. Wave-induced bottom stress at a water depth of 30 m was chosen as representative of Massachusetts Bay (about 45% of Massachusetts Bay, defined as the region to the west of a line from Cape Ann to the outer edge of Cape Cod, is shallower than 30 m); stress would be higher in shallower areas and lower in deeper areas. Wave stress was also computed at 80 m water depth, typical of the deep areas of Massachusetts Bay in Stellwagen Basin (Fig. 1). For records 374 and 413 obtained at LT-A, the full bottom wave-current stress was computed using Madsen (1994) and currents and waves measured 1 m above bottom and a physical roughness of 0.05 m.

4. Defining metrics for storm strength

A storm based on wind stress was defined as a period when wind stress exceeded 0.2 Pa (about 11 m/s, 22 knots, or 25 mph) for at least 6 h. On the Beaufort scale, this wind speed is equivalent to a Strong Breeze and is 3 m/s less than a Gale. Wind stress had to fall below 0.2 Pa for at least 12 h to initiate a new storm. Integrated wind stress (hereafter called IWINDS) was defined as the sum of the magnitudes of the hourly wind stress for the duration of the storm. Vector-averaged wind stress was computed over the duration of the IWINDS event. The wind direction is the direction from which the wind blows. The average of the three largest hourly wind stresses during each storm was determined as a measure of the maximum wind stress. Statistics of the largest 25 storms ranked by IWINDS are listed in Table 1.

A storm based on bottom-wave stress at a water depth of 30 m was defined as a period when the bottom stress caused by waves was greater than 0.1 Pa for at least 6 h. Wave stress had to fall below 0.1 Pa for at least 12 h to initiate a new storm. An integrated excess bottom stress caused by waves (hereafter called IWAVES) was defined as the sum of the magnitude of the bottom stress, minus the threshold of 0.1 Pa, for the duration of the storm. (Note that IWAVES is the equivalent of Integrated Excess Stress (IES) used in Warner et al., 2008.) The vector-averaged wind stress was computed over the duration of the IWAVES event. However, wind stress determined over the duration of the IWINDS event is a better measure of the storm wind stress because IWAVES events often include a period with large waves but weaker wind stress after the storm has passed. The average of the three largest hourly wave stresses during each storm was determined as a measure of the maximum stress. Statistics for the largest 25 storms ranked by IWAVES are listed in Table 2a. Statistics of the wave current and stress calculated at 80 m water depth for the same 25 storms are listed in Table 2b.

A bottom stress of 0.1 Pa is used as the threshold to define a storm on the sea floor. This is the stress required to initiate motion of very fine sand (quartz grains of 0.08 mm diameter) in seawater (White, 1970) and is taken as an approximate threshold for resuspension of fine-grained sediments typical of Massachusetts Bay. Kalnejais et al. (2007) made measurements of sediment resuspension at a site in western Massachusetts Bay at a water depth of about 30 m and found that a stress of about 0.12 Pa initiated resuspension. A stress of about 0.12 Pa to resuspend fine-grained sediments was also inferred from current observations

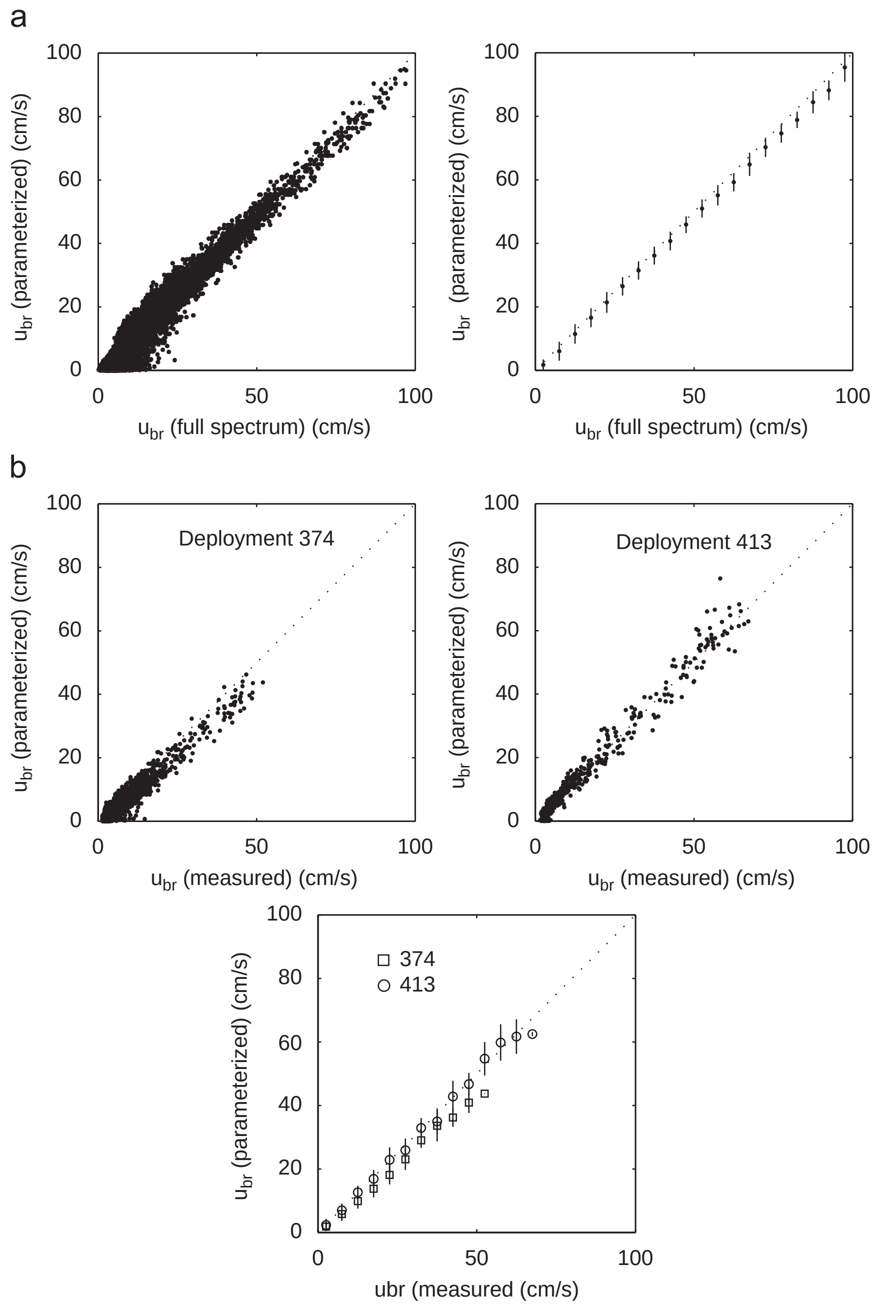

Fig. 2. (a) Near-bottom wave-orbital velocities (u_{br}) at a water depth of 30 m, computed from surface-wave spectra at NDBC 44013, compared to u_{br} at 30 m computed by the parametric spectral method of Wiberg and Sherwood (in press) from H_s and T_p. The scatterplot on the left shows all observations individually; the plot on the right shows wave-orbital velocities binned in 5 cm/s intervals, and error bars indicate one standard deviation around the bin-averaged values. These data were obtained from the 3 m discus buoy from 1997 through 2006. (b) Near-bottom wave-orbital velocities (u_{br}) measured 1 m above bottom at LT-A (Fig. 1) compared to u_{br} computed by the parametric method using surface H_s and T_p observations (as in Fig. 2a). Observations are shown for deployment 374 (February–June 1991) and 413 (circles) (deployed from February to March 1993). The current measurements were made 1 m above bottom by using a BASS (Benthic Acoustic Stress Sensor) sampling at 2 Hz for 450 s each hour; u_{br} was computed as the sum of the variance of the east and north current components, and the period was determined from the zero-crossing of the east–west current component during each burst (see Butman et al. (2004) for a description of measurements). Error bars represent one standard deviation.

obtained in Stellwagen Basin (at a water depth of about 80 m) (Butman et al., 2006). (Note that 0.12 Pa is a factor of two larger than the estimate given in Butman et al. (2006) because of an erroneous factor of 0.5 in the drag formula they used to estimate bottom stress from near-bottom current.) There is considerable variability and uncertainty in any sediment-resuspension threshold, and a single threshold certainly does not apply to all sediments during all seasons. The choice of threshold that defines a storm affects the number and duration of the storms (Table 3), but does not alter the ranking of the largest events or the seasonal and interannual distribution of storms. The threshold of 0.1 Pa is of the right order for fine-grained sediments, and the selection of a round number for the threshold is intended to convey a conical number.

5. Results

5.1. Largest storms

The largest storm ranked by IWAVES and IWINDS was the Blizzard of 1992 in December 1992 (Fig. 3a; Tables 1, 2a, and 2b).

Table 1
Statistics of the 25 (5% of the total no. of storms defined by wind stress) strongest storms between 1990 and 2006, ranked by the integrated wind stress greater than 0.2 Pa (IWINDS)

Wind rank	Wave rank	Start	Duration (h)	IWINDS (Pa h)	Average wind stress magnitude (Pa)	Maximum wind stress magnitude (Pa)	Vector-averaged wind stress	
							Magnitude (Pa)	Direction (°)
1	1	10 December 1992	83	55	0.67	1.19	0.62	57
2	2	28 October 1991	102	43	0.42	1.06	0.42	24
3	3	5 December 2003	62	35	0.57	1.28	0.50	13
4	–	25 December 2000	92	32	0.35	0.72	0.35	285
5	264	10 November 1990	88	31	0.35	0.63	0.28	266
6	–	20 January 2003	84	28	0.34	0.60	0.33	270
7	–	15 January 1994	111	28	0.25	0.51	0.20	275
8	17	23 December 1994	48	27	0.57	1.19	0.57	9
9	14	23 May 2005	70	27	0.38	0.69	0.37	26
10	6	22 January 2005	39	26	0.68	1.29	0.58	7
11	70	4 February 1995	67	25	0.38	0.86	0.22	264
12	29	16 November 2002	64	24	0.38	0.72	0.23	3
13	124	20 January 2000	52	24	0.47	0.68	0.40	299
14	73	20 December 1995	71	24	0.34	0.58	0.26	311
15	7	11 December 1993	82	24	0.29	0.60	0.26	354
16	–	6 January 1997	70	22	0.32	0.63	0.31	277
17	31	25 December 2002	45	22	0.48	0.97	0.33	341
18	–	13 November 2003	58	21	0.37	0.65	0.36	276
19	215	28 October 2006	57	21	0.37	0.70	0.20	214
20	18	24 February 1998	68	21	0.31	0.65	0.24	351
21	8	31 March 1997	30	21	0.68	1.01	0.66	18
22	68	6 March 1999	64	21	0.33	0.62	0.27	327
23	–	15 January 2006	53	20	0.38	0.67	0.37	307
24	24	7 May 2005	48	20	0.42	0.73	0.42	4
25	95	16 January 2000	42	20	0.48	0.96	0.37	297

Wind rank is based on IWINDS and wave rank is based on IWAVES (Table 2). Maximum wind stress magnitude is the average of the three largest wind stresses during the storm. Wind stress is vector-averaged wind stress over the duration of the storm defined by wind stress >0.2 Pa. Direction is from which the wind blows (0–90 is from the northeast). (–) Storm did not rank as an IWAVES event.

Table 2a
Statistics of the 25 (7% of the total no. of storms) strongest storms between 1990 and 2006, ranked by the integrated excess bottom-wave stress greater than 0.1 Pa (IWAVES) at a water depth of 30 m

Wave rank	Wind rank	Start time	Storm duration (h)	Surface waves		Wave statistics calculated at 30 m water depth				Vector-averaged wind stress	
				Average H_s (m)	Average T_p (s)	Average u_{br} (m/s)	Average τ_{bw} (Pa)	Maximum τ_{bw} (Pa)	IWAVES (Pa h)	Magnitude (Pa)	Direction (°)
1	1	11 December 1992	146	4.0	12.6	0.48	1.20	3.11	160	0.33	54
2	2	28 October 1991	128	3.7	11.4	0.42	1.01	5.23	116	0.33	24
3	3	6 December 2003	89	4.6	10.9	0.49	1.38	3.86	114	0.37	9
4	*	5 March 2001	123	4.0	11.7	0.41	0.99	2.96	109	*	*
5	35	28 January 1998	254	2.5	10.9	0.23	0.38	1.46	72	0.14	14
6	10	23 January 2005	52	4.7	11.3	0.50	1.34	3.36	65	0.44	359
7	15	11 December 1993	186	3.0	10.6	0.26	0.44	1.27	63	0.21	7
8	21	31 March 1997	76	3.8	10.1	0.38	0.86	3.00	56	0.3	4
9	30	23 October 2005	101	3.3	10.5	0.31	0.63	2.87	53	0.21	5
10	42	19 October 1996	141	2.8	10.9	0.28	0.49	1.55	52	0.11	71
11	31	4 March 1993	85	3.5	11.8	0.37	0.79	2.01	52	0.24	44
12	81	20 October 2004	242	2.5	10.4	0.21	0.31	0.94	51	0.11	21
13	92	2 January 2003	95	3.5	9.9	0.32	0.62	2.01	49	0.21	20
14	9	22 May 2005	135	3.0	9.9	0.27	0.46	1.27	49	0.22	22
15	57	16 January 1998	156	2.7	10.9	0.26	0.41	1.12	48	0.18	359
16	37	26 December 2004	60	4.0	11.0	0.35	0.81	2.35	43	0.3	351
17	8	23 December 1994	80	3.7	9.3	0.30	0.59	2.04	39	0.4	6
18	20	24 February 1998	108	2.7	12.2	0.27	0.46	1.62	38	0.18	346
19	98	19 April 1997	52	3.6	10.6	0.38	0.84	2.90	38	0.23	13
20	40	8 January 1996	144	2.6	10.0	0.22	0.35	1.46	36	0.16	352
21	250	28 February 1993	57	3.2	12.3	0.34	0.69	2.17	34	0.13	348
22	83	17 March 2000	182	2.2	10.3	0.20	0.28	0.89	32	0.1	11
23	86	21 March 1998	61	3.5	9.8	0.31	0.62	1.71	31	0.19	28
24	24	7 May 2005	75	3.0	9.7	0.27	0.47	1.25	27	0.26	3
25	–	2 February 2005	154	2.0	11.1	0.20	0.27	0.60	27	0.05	16

Wave rank is based on IWAVES and wind rank based on IWINDS (Table 1). Wind stress is vector-averaged over the duration of the storm defined by wave-bottom stress greater than 0.1 Pa. Direction is from which the wind blows (0–90 from the northeast). Maximum τ_{bw} is the average of the three largest bottom-wave stresses during the storm. Table 2b contains companion wave statistics computed at 80 m.

* Wind data not available for this storm. (–) Not ranked as an IWINDS event.

Table 2b
Wave statistics at 80 m water depth of the 25 (7% of the total no. of storms) strongest storms between 1990 and 2006, ranked by the integrated excess bottom-wave stress greater than 0.1 Pa (IWAVES) at a water depth of 30 m

Wave rank	Start time	Wave statistics calculated at 80 m water depth				
		Duration $\tau_{bw} > 0.1$ Pa (h)	Average u_{br} (m/s)	Average τ_{bw} (Pa)	Maximum τ_{bw} (Pa)	IWAVES (Pa h)
1	11 December 1992	83	0.14	0.16	0.47	12.2
2	28 October 1991	43	0.12	0.15	1.09	11.4
3	6 December 2003	40	0.13	0.16	0.60	8.6
4	5 March 2001	50	0.11	0.11	0.36	6.7
5	28 January 1998	15	0.05	0.04	0.16	0.5
6	23 January 2005	25	0.13	0.14	0.39	3.6
7	11 December 1993	12	0.06	0.04	0.14	0.2
8	31 March 1997	23	0.09	0.08	0.34	2.2
9	23 October 2005	18	0.07	0.06	0.34	2.0
10	19 October 1996	8	0.06	0.04	0.14	0.2
11	4 March 1993	32	0.10	0.09	0.24	2.3
12	20 October 2004	10	0.05	0.03	0.12	0.1
13	2 January 2003	14	0.07	0.05	0.25	0.8
14	22 May 2005	7	0.05	0.04	0.12	0.1
15	16 January 1998	6	0.06	0.04	0.13	0.1
16	26 December 2004	22	0.09	0.08	0.31	2.1
17	23 December 1994	10	0.06	0.04	0.19	0.4
18	24 February 1998	9	0.07	0.05	0.15	0.2
19	19 April 1997	13	0.09	0.08	0.33	1.4
20	8 January 1996	6	0.04	0.03	0.13	0.1
21	28 February 1993	20	0.10	0.10	0.39	2.5
22	17 March 2000	0	0.04	0.02	0.08	0
23	21 March 1998	11	0.06	0.05	0.16	0.4
24	7 May 2005	4	0.05	0.04	0.11	0
25	2 February 2005	0	0.05	0.03	0.08	0

Maximum τ_{bw} is the average of the three largest bottom-wave stresses during the storm.

Table 3
Grain size resuspended (critical stress from White (1970)), no. of storms, storm duration, and total IWAVES at 30 and 80 m water depth for the period 1990–2006 for critical stresses between 0.06 and 0.14 Pa

Critical stress (Pa)	$u^*_{critical}$ (cm/s)	Grain size resuspended (Phi)	No. of storms (average storms/year)		Average storm duration (range) (h)		Total IWAVES (range each event) (Pa h)	
			30 m	80 m	30 m	80 m	30 m	80 m
0.06	0.8	5	539 (32)	73 (4)	53 (7–393)	16 (1–92)	3833 (0.0–165)	90 (0.0–15)
0.10	1.0	4	380 (22)	41 (2)	47 (7–254)	14 (1–83)	3152 (0.0–160)	60 (0.0–12)
0.12	1.1	3.4	337 (20)	36 (2)	42 (7–226)	12 (1–78)	2862 (0.0–157)	50 (0.0–11)
0.14	1.2	3	297 (18)	24 (1)	39 (7–219)	14 (1–73)	2598 (0.1–154)	42 (0.0–10)

This paper uses a critical stress of 0.1 Pa to define IWAVES events. Phi is $-\log_2$(grain diameter in mm).

This storm was about 40% larger than the next largest storms, based on IWAVES at a depth of 30 m, in October 1991 (the Perfect Storm described by Junger (1997)) (Fig. 3b), December 2003, and March 2001 (Tables 1, 2a, and 2b). These storms were all northeasters, with vector-averaged winds from the northeast (Tables 1, 2a, and 2b). The December 1992 storm (Fig. 3a) had wind stress exceeding 1 Pa (wind speeds in excess of 20 m/s), significant wave heights in excess of 5 m, wave-orbital velocities at 30 m water depth in excess of 1 m/s, and wave bottom stress greater than 3 Pa; it lasted about 146 h, as defined by bottom stress at 30 m water depth, 63 h longer than the duration defined by wind stress (Tables 1, 2a, and 2b). The October 1991 storm (Fig. 3b) had significant wave heights in excess of 9 m, wave-orbital velocities at 30 m water depth in excess of 1.2 m/s, and wave-generated bottom stress greater than 5 Pa; the storm lasted about 128 h. If storms were ranked by maximum bottom-wave stress, the October 1991 storm, December 2003 and January 2005 storms would rank before the December 1992 storm (Table 2a).

5.2. *Storms defined by integrated wind stress*

There were 515 storms (about 30 per year) defined by IWINDS during the period 1990–2006 (Figs. 4a and 5). The strongest storms had vector-averaged wind stress from the northeast through west quadrants (Fig. 4b). Ninety-five percent of the storms had IWINDS less than 20 Pa h, and 70% had IWINDS less than about 8 Pa h (Fig. 4e). The typical average wind speed during the IWINDS storms ranged from 10 to 15 m/s (Fig. 6a). The typical average wind stress ranged from 0.2 to 0.4 Pa (Fig. 6b) and the maximum wind stress ranged from 0.2 to 1.0 Pa (Fig. 6c). The duration of storms was typically less than 2 days, with only a few storms lasting longer than 4 days (Fig. 6d). The number of storms defined by IWINDS ranged from about six per month in winter to less than one per month in summer and the percentage of time that the wind exceeded 0.2 Pa was about 20% of the time in winter and less than 1% of the time in summer (Fig. 7).

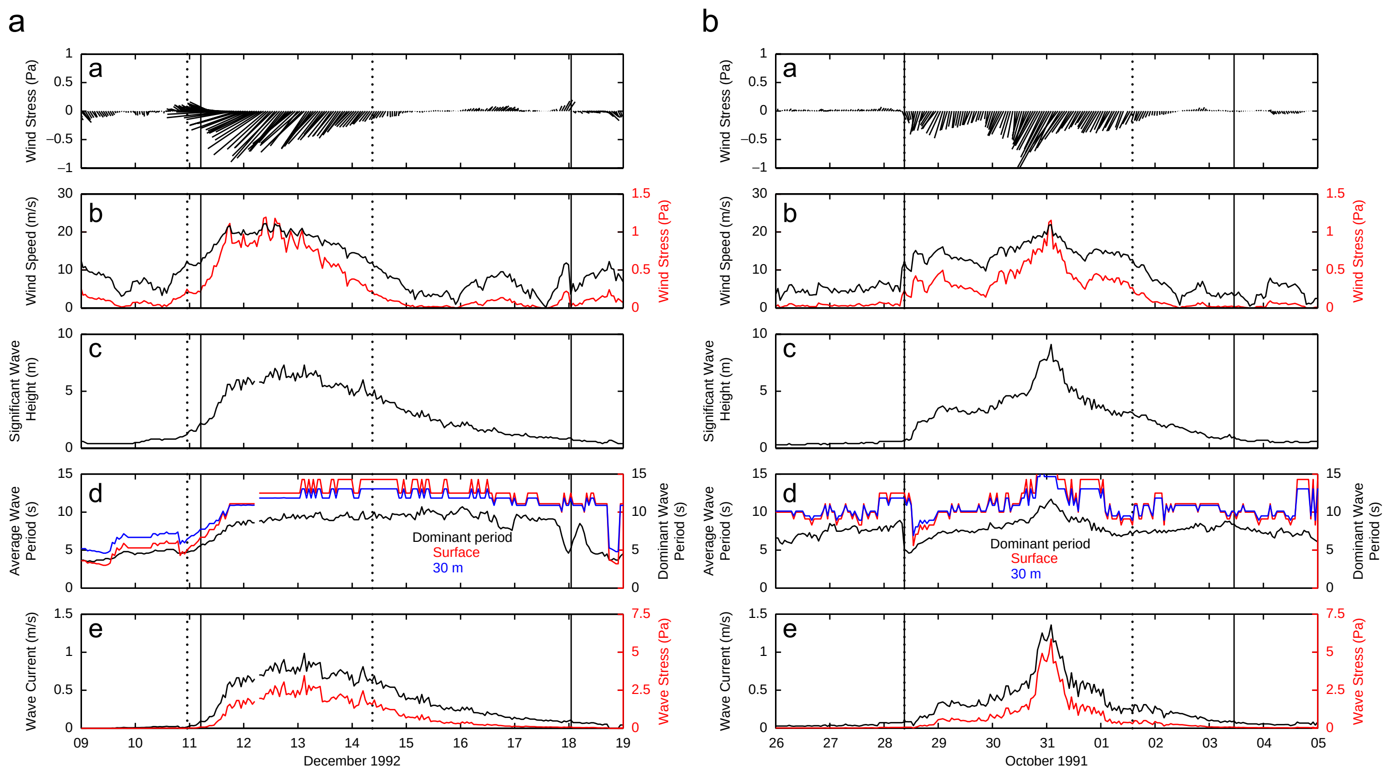

Fig. 3. (a) Time-series plot of wind and wave observations from NDBC 44013 for the December 1992 storm, the strongest storm during the period 1990–2006 as defined by IWINDS and IWAVES: (a) hourly wind stress (sticks point toward the direction the wind blows); (b) wind speed and wind stress magnitude; (c) significant wave height; (d) average and dominant (at surface in red, at 30 m water depth in blue) wave period; (e) bottom wave-orbital current and bottom-wave stress. The vertical solid lines indicate the limits of the storm defined by wave stress (at a depth of 30 m) greater than 0.1 Pa; the vertical dotted lines indicate the limits of the storm defined by wind stress greater than 0.2 Pa. (b) Time-series plot of wind and wave observations from NDBC 44013 for the October 1991 storm, the second strongest storm during the period 1990–2006 as defined by IWINDS and IWAVES. See (a) for description.

The strongest 25 storms ranked by IWINDS (5% of the total) occurred in the months of October–May (Table 1; Fig. 8a); none of the 25 strongest storms occurred during the months June, July, August, and September. The average magnitude of the wind stress during the strongest 25 storms ranged from 0.25 to 0.67 Pa (Fig. 8b; Table 1). Of the 25 largest storms ranked by IWINDS, nine had wind stress from the northeast quadrant (vector-averaged stress from between 0° and 90°) (Table 1; Fig. 8). Of these nine strongest northeasters ranked by IWINDS, seven occurred in fall or winter (one in October, one in November, three in December, one in January, one in March) and two in spring (May). The two strongest northeast storms were the Blizzard of 1992 (10–14 December 1992) and the Halloween or Perfect Storm (28 October–1 November 1991). Three of the nine strongest northeast storms ranked by IWINDS occurred in 2005, one in January and two in May.

5.3. *Storms defined by integrated bottom-wave stress*

There were 380 storms (about 22 per year) defined by IWAVES during the period 1990–2006 (Figs. 4b and 5). Ninety-five percent of the storms had IWAVES less than about 40 Pa h, and 70% had IWAVES less than about 5 Pa (Fig. 4e). The strongest events defined by IWAVES are associated with winds from about 0° to 60° (generally from the northeast) (Fig. 4d). Average significant wave height during IWAVE events ranged from 0.5 to 4.7 m (Fig. 6e) and dominant wave period from 7 to 15 s (Fig. 6f). Wave-generated bottom stress at 30 m ranged from 0 to 1.5 Pa (Fig. 6g) and maximum 3-h stress ranged from 0 to 4 Pa (Fig. 6h). The duration of storms was typically less than 6 days (Fig. 4i). The number of storms defined by IWAVES ranged from about three per month in winter to less than one per month in summer (Fig. 7a). Wave stress at 30 m exceeded 0.1 Pa about 15% of the time in winter and less than 0.5% of the time in summer (Fig. 7b).

The strongest 25 storms (about 7% of the total) ranked by IWAVES occurred in the months of October–May; none of these storms occurred in the months June–September (Fig. 8c). The average bottom stress during the 25 strongest storms ranked by IWAVES ranged from about 0.27 to 1.4 Pa (Fig. 8d; Tables 2a and 2b).

The sum of IWAVES from October through May, a measure of the cumulative sediment reworking by waves during storms during the winter season, ranged by about a factor of 11 (Fig. 9; Table 4). The winters of 1992–1993, 1997–1998, and 2004–2005 were the strongest and the winter of 2001–2002 was the weakest. On average there were about 19 IWAVE events and 29 IWIND events over this 8-month winter period.

6. Discussion

The integrated bottom stress at a selected water depth (IWAVES) is a measure of the ability of a storm to rework and resuspend sediments on the sea floor. IWAVES (and IWINDS) are analogous to the storm power, defined by Dolan and Davis (1992) as storm duration multiplied by the square of significant wave height. IWAVES combines storm duration and intensity into a single metric. A different metric might be more appropriate than the integrated stress for some bottom processes. For example,

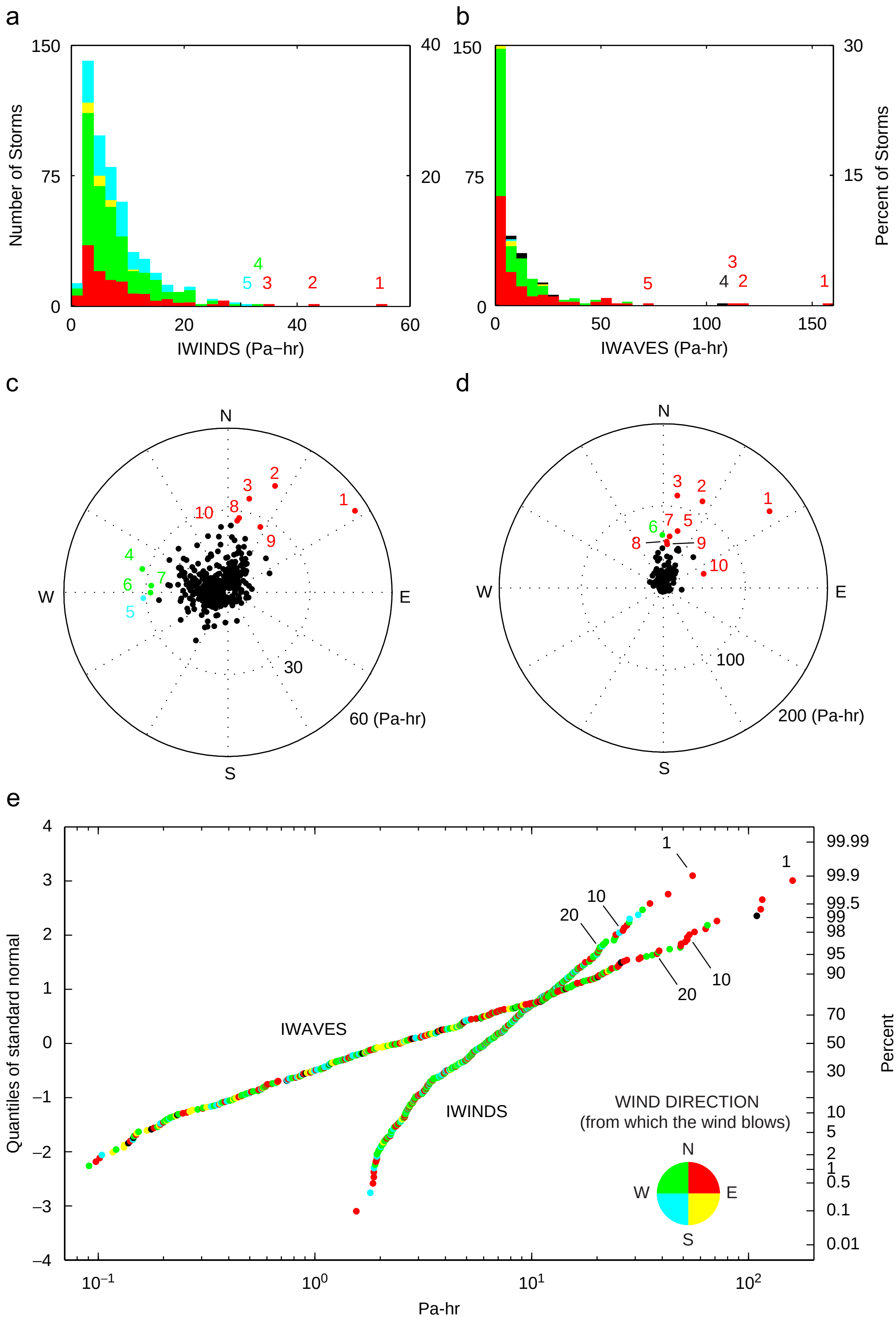

Fig. 4. Statistics of integrated wind stress (IWINDS) and wave stress (IWAVES) at 30 m water depth: (a) histogram of IWINDS (5 largest numbered); (b) histogram of IWAVES (5 largest numbered; lowest bin is truncated and does not show all southeast or southwest occurrences); (c) polar scatterplot of IWINDS and vector-averaged wind-stress direction (10 largest storms colored by wind stress direction and rank labeled); (d) polar scatterplot of IWAVES and vector-averaged wind-stress direction (10 largest storms colored by wind stress direction and rank labeled). Wind data were not available for the 4th largest storm (Tables 2a and 2b) and thus not shown. (e) Normalized IWINDS and IWAVES (mean subtracted and divided by the standard deviation) on a log plot; the straight line indicates the distributions shown in (a) and (b) are log-normal. Storms ranked 1, 10, and 20 (Tables 1, 2a, and 2b) are labeled. Wind direction of each storm is vector-averaged direction from which the wind blows, and is coded by color: red (from the northeast), yellow (from the southeast), cyan (from the southwest), and green (from the northwest).

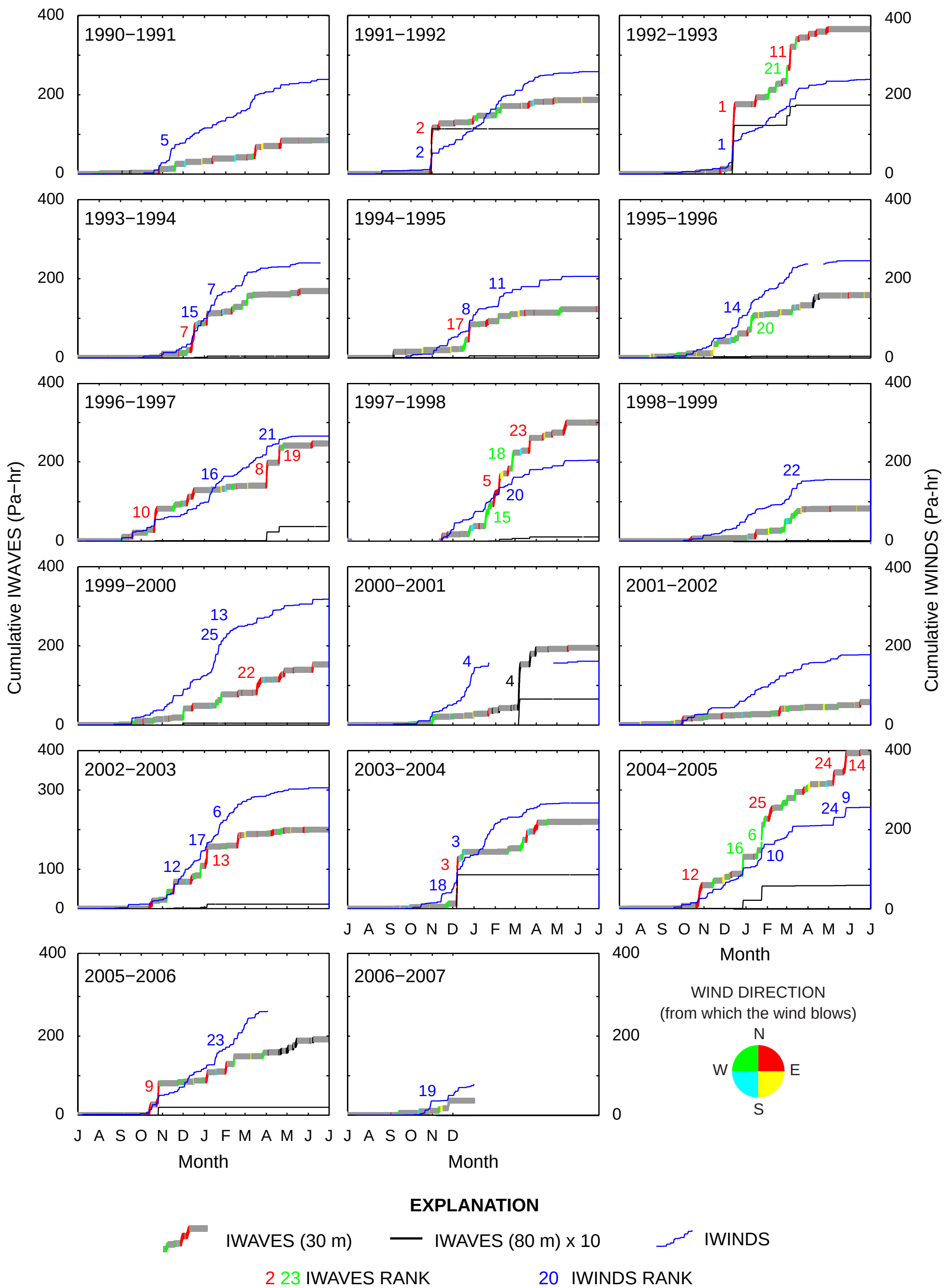

Fig. 5. Time-series of cumulative wind stress (IWINDS) (blue line) and cumulative excess bottom-wave stress at a water depth of 30 m (IWAVES) (thick line; colors other than gray represent the vector-averaged wind stress direction during IWAVE storms and gray represents other times) and at a depth of 80 m (black; multiplied by 10) for the years 1990–2006. Wave stress was calculated from significant wave height and dominant wave period following the method of Wiberg and Sherwood (in press) based on the Donelan spectrum. Numbers are the ranks of the strongest 25 storms defined by IWAVES (numbers colored by wind stress direction: red (from northeast), yellow (from southeast), cyan (from southwest), and green (from northwest)) and by IWINDS (numbers in blue) (Tables 1, 2a, and 2b). The wind-stress direction during IWAVES events is the vector-averaged wind stress over the entire event; the varying wind direction during IWAVES events cannot be shown at this scale.

maximum stress during a storm might be appropriate if the depth of sediment erosion or mobilization of a mixed sediment layer was the process of interest. On the basis of the average of the three strongest wave-bottom stresses during a storm, the October 1991, December 2003, and January 2005 storms were all stronger than the December 1992 storm (Table 2a). However, the main objective

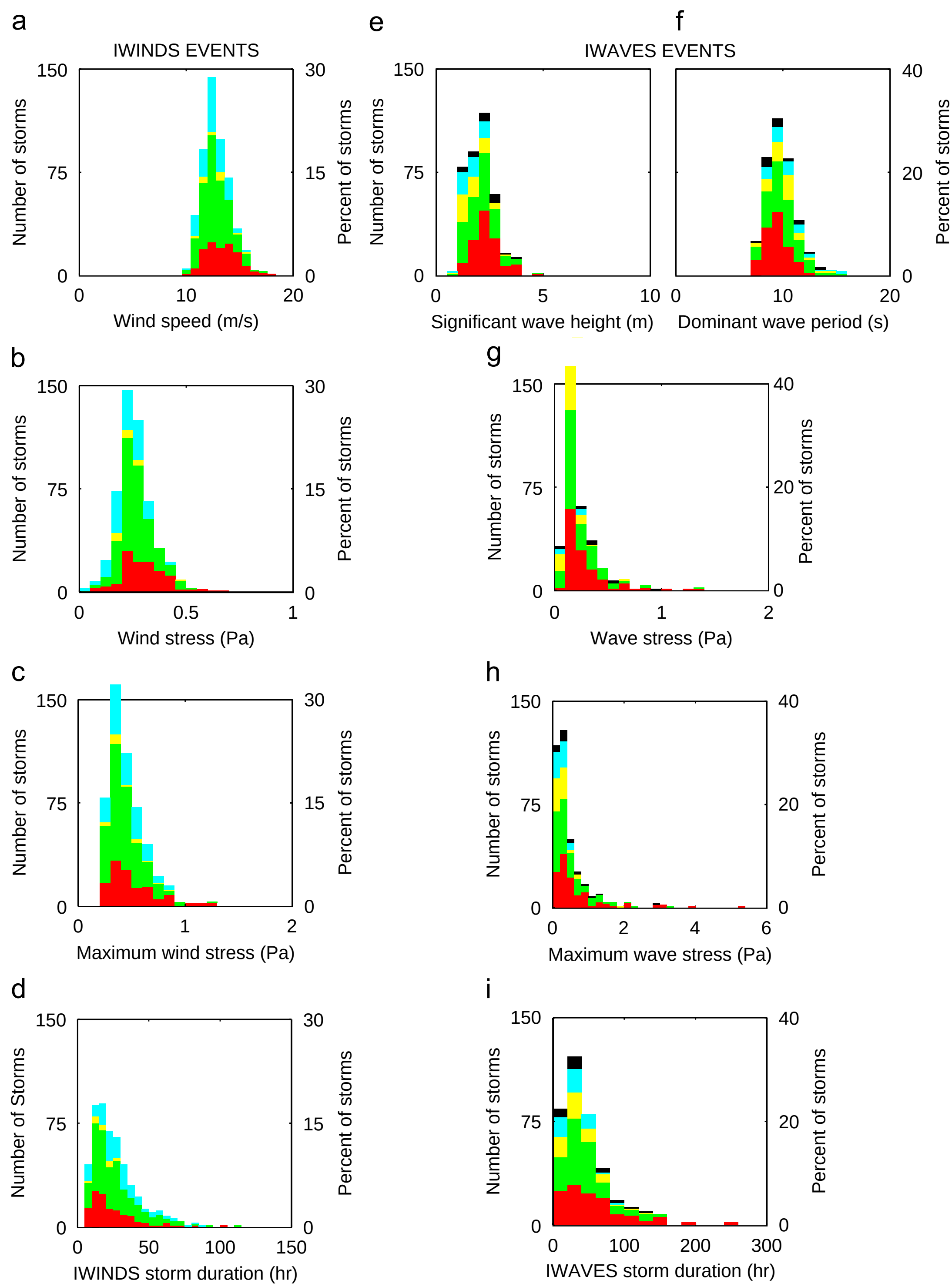

Fig. 6. Histograms of characteristics for each of the 515 storms defined by IWINDS (panels a–d) and the 380 storms defined by IWAVES at 30 m water depth (panels e–i) from January 1990 through December 2006: (a) average wind speed; (b) average wind stress magnitude; (c) average of largest three wind stresses during each storm; (d) storm duration defined by wind stress; (e) average significant wave height; (f) average dominant wave period; (g) average wave stress at 30 m water depth; (h) average of largest three wave stresses during each storm; (i) storm duration defined by wave stress. Colors for wind directions from which the wind blows are: red (from northeast), yellow (from southeast), cyan (from southwest), and green (from northwest). Black indicates no wind direction available.

of this paper is to introduce the concept of a metric for storms on the sea floor based on bottom stress; the details may be adjusted for the process of interest.

The IWAVES metric uses bottom stress caused by surface-wave-generated currents that are calculated from long-term buoy observations. In reality, these wave currents are superimposed on tidal and wind-driven currents that would increase the bottom stress from that caused by the wave currents alone. Long-term continuous measurements of near-bottom currents are not available. The addition of tidal and wind-driven currents to the

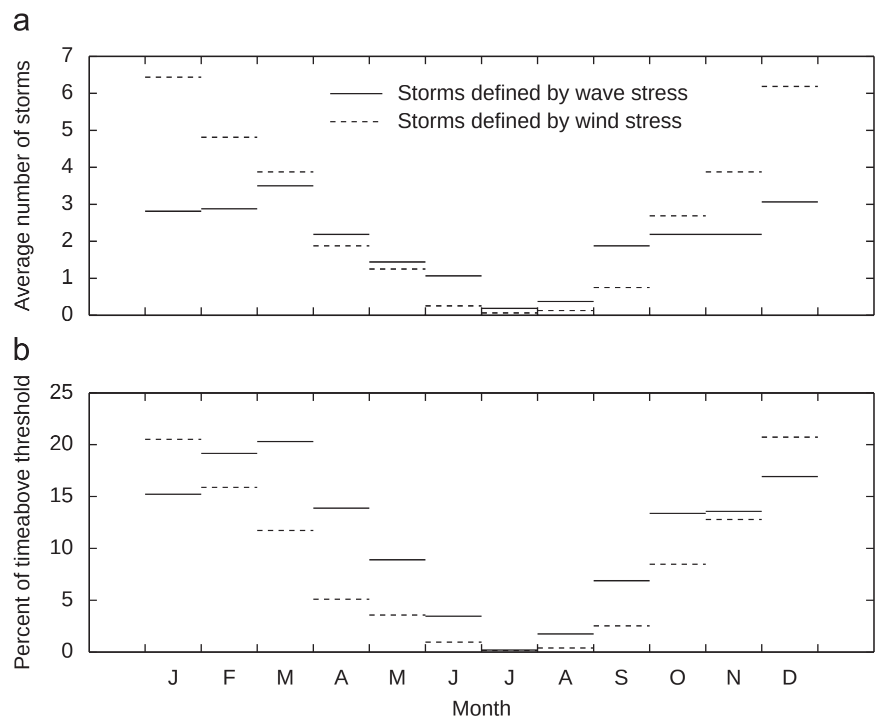

Fig. 7. (a) Average number of storms starting each month defined by IWINDS (dashed line) and IWAVES (solid line) for the period 1990–2006. (b) Average percent of time per month that wind stress exceeded 0.2 Pa (IWINDS) and wave stress exceeded 0.1 Pa (IWAVES).

bottom-stress calculation could be accomplished using predictions from a numerical model. This would add significant complexity to the stress calculation, however, and the bottom-wave stress captures the dominant cause of sediment resuspension associated with storms in Massachusetts Bay and on many continental shelves. For example, for records 374 and 413 at LT-A obtained in 1993 and 1996, respectively, the ratio of the wave stress to the wave-current stress exceeded 0.8 during storm events, indicating that waves are the major contributor to the total stress.

Wiberg et al. (2002) used 17 years of buoy data to estimate sediment resuspension and transport on the Palos Verdes Shelf offshore of California. Because the waves and near-bottom currents were uncorrelated at this location, Wiberg et al. constructed a representative 10.5-month time-series of bottom current from observations and combined them with the buoy wave measurements to compute bottom stress over the 17-year interval. This is another strategy, applicable to some locations, to incorporate representative currents into the bottom stress calculation where long-term current observations are not available.

IWAVES is a measure of wave-bottom stress based on measurements at a single location; the characteristics of surface waves at a particular location are a function of wind speed, storm path, and the speed of travel of a storm system, as well as the regional and local topography. The waves measured at buoy 44013 in Massachusetts Bay probably are representative of the waves over a broad area of Massachusetts Bay and the western Gulf of Maine. IWAVES computed from the this buoy however, is not a good measure of storm effects on the sea floor in Cape Cod Bay or Boston Harbor; these areas are not exposed to the same wave field because of the coastline geometry.

A full description of the surface-wave spectrum is usually required for an accurate calculation of the near-bottom wave-orbital velocities and stress caused by the surface-wave field (Madsen, 1994). The use of H_s and T_p, or H_s and T_{av}, in a simple monochromatic formula for depth-dependent orbital decay produces poor estimates of near-bottom wave-orbital velocity (Soulsby, 1987). When H_s and T_p are available, however, a parametric formulation of the wave spectrum can be used to estimate near-bottom wave-orbital velocities (Wiberg and Sherwood, in press). This method was used to calculate near-bottom orbital speeds in Massachusetts Bay from 1990 to 1996 when full spectra were not available. Although NDBC wave observations were started in Massachusetts Bay in 1984, 1990 was chosen as the start date for the analysis described in this paper because of gaps in the wave record between 1984 and 1990.

The characteristics of storms defined by IWAVES differ with the selection of water depth and critical bottom stress. Storms by this metric would be more frequent and longer for a shallower depth or lower threshold and less frequent and shorter for a greater depth or higher threshold (Table 3). For example, for a threshold of 0.1 Pa, there were about 22 storms/year with an average duration of 47 h at depth of 30 m, but only 2 storms/year with an average duration of 14 h at a depth of 80 m. The overall percentage of time that wave-generated bottom stress exceeds 0.1 Pa ranges from about 11% at a depth of 30 m, to less than 1% at a depth of 80 m (Fig. 10). We somewhat arbitrarily chose 30 m as the water depth for the IWAVE calculations for Massachusetts Bay; about 45% of the Bay is shallower than 30 m and the crest of Stellwagen Bank and a transition from coarse to finer grained sediments in western Massachusetts Bay occurs at the 30–40 m isobath. We also included IWAVES calculations at 80 m characteristic of Stellwagen Basin, the deepest area of Massachusetts Bay.

The Blizzard of 1992 (December 1992), the Perfect Storm (October 1991), and a December 2003 storm are the three strongest storms ranked by both IWINDS and IWAVES for the period 1990–2006. All three storms were northeasters, with vector-averaged wind stress from 55°, 23°, and 4°, respectively. No wind records were available from NDBC 44013 for the fourth strongest storm ranked by IWAVES (March 2001), but weather maps (National Oceanic and Atmospheric Administration National

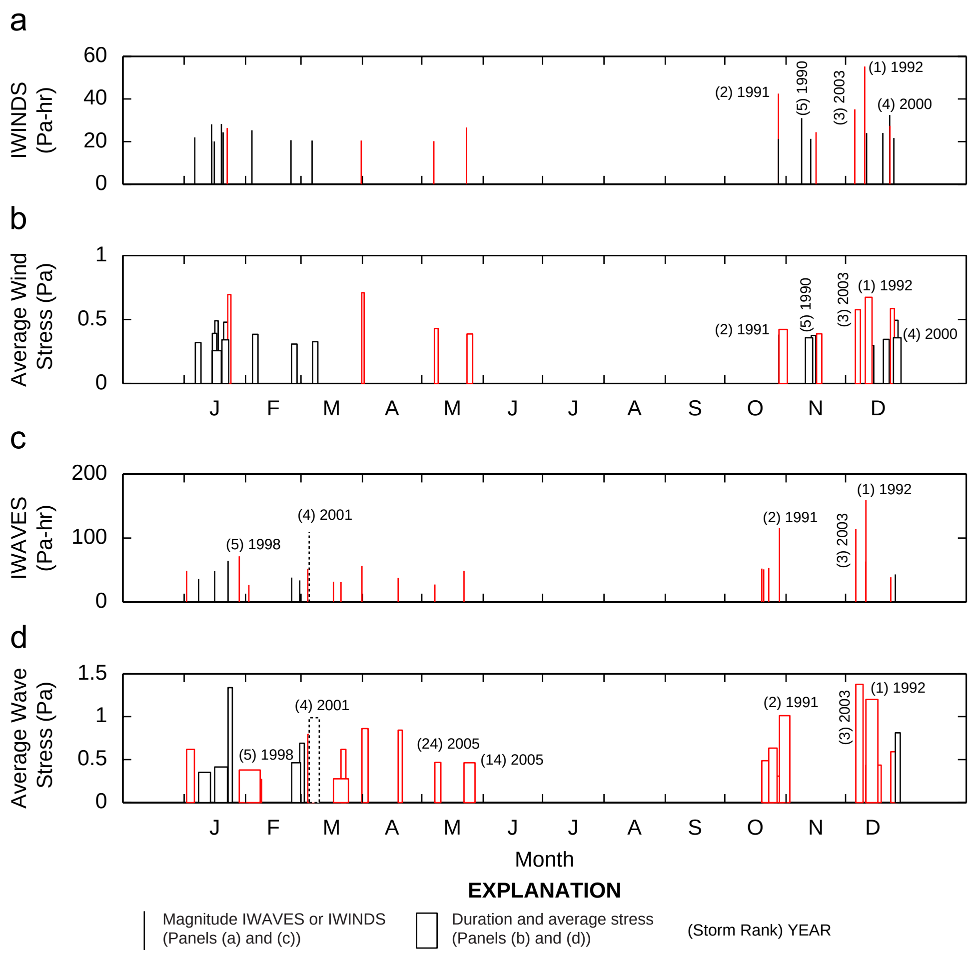

Fig. 8. Occurrence by month of the largest 25 storms from January 1990 through December 2006 ranked by IWINDS (panels a and b) and IWAVES at 30 m water depth (panels c and d). (a) Magnitude of IWINDS of the largest 25 storms ranked by IWINDS (bar plotted at the start time of the storm). (b) Average wind stress during the 25 largest storms ranked by IWINDS. The width of the bar represents storm duration; the area of the bar represents the magnitude of IWINDS. (c) Magnitude of IWAVES of the largest 25 storms ranked by IWAVES (bar plotted at the start time of the storm). (d) Average wave stress at 30 m water depth during the largest 25 storms ranked by IWAVES. The width of the bar represents the storm duration; the area of the bar represents the magnitude of IWAVES. Storms with vector-averaged wind stress from the northeast quadrant (0–90°) are shown in red. There were no wind observations during the March 2001 storm and it is shown as a dashed line. The five largest storms are labeled by rank (in parentheses) and year.

Weather Service, 2001) show this was a northeaster as well. Of the storms in the top 10% ($n = 38$) ranked by IWAVES, 22 had vector-averaged wind stress from the northeast quadrant (winds from 0° to 90°), 12 from the north-northwest quadrant (between 337° and 360°), and 2 from the southeast quadrant (2 did not have wind observations). Northeasters are clearly the major cause of large waves in Massachusetts Bay.

Some of the large IWAVE events have vector-averaged wind stress from the north-northwest quadrant—for example the storms in January 2005, January 1998, December 2004, and February 1998 (Fig. 5; Table 2a)—that at first seems inconsistent with northeasters. Despite the northwest wind direction, however, these large events are northeasters. In these storms the center of the low-pressure system passed to the south of Massachusetts Bay; although winds were from the north over the Bay, they were from the northeast over the Gulf of Maine, especially once the storm center passed to the southeast. In this storm geometry, although the wind stress measured at 44013 averaged over the storm was from the north-northwest, the long-period large waves that affected the sea floor in Massachusetts Bay were created by winds blowing from the northeast over the Gulf of Maine. A more appropriate wind metric might be one that integrates over the region of wave generation, but this is not feasible with available measurements.

Of the top 10% (51) largest storms ranked by IWINDS, 16 had wind stress from the northeast quadrant (vector-averaged stress from between 0° and 90°). Of these 16 strongest northeasters ranked by IWINDS, 13 occurred in fall or winter (1 in September, 3 in October, 1 in November, 3 in December, 2 in January, 1 in February, and 2 in March) and 3 in spring (May) (Fig. 8). Four of the 16 strongest northeast storms occurred in 2005, 1 in January, 2 in May, and 1 in October.

The duration of storms defined by IWAVES was considerably longer than storms defined by IWINDS (Fig. 6d and i; Tables 1, 2a, and 2b). This reflects waves generated in the Gulf of Maine that propagate into Massachusetts Bay as the storm systems travel northeastward and after local winds have decreased. For example, the December 1992 storm was 165 h long based on the wave bottom-stress criteria but only 83 long hours based on the wind-stress criteria. In these cases, the vector-averaged wind over an IWAVE storm sometimes included weaker post-storm winds.

Some notable large storms moved too fast, or the storm path and wind field were such that they did not generate large waves in Massachusetts Bay, and thus they did not rank high in the IWAVES or IWINDS ranking. For example, Hurricane Bob (19 August 1991) was the only hurricane between 1990 and 2006 that affected Massachusetts. The hurricane passed through the region in less than 1 day; it ranked 206 in IWINDS (duration 12 h) and did not

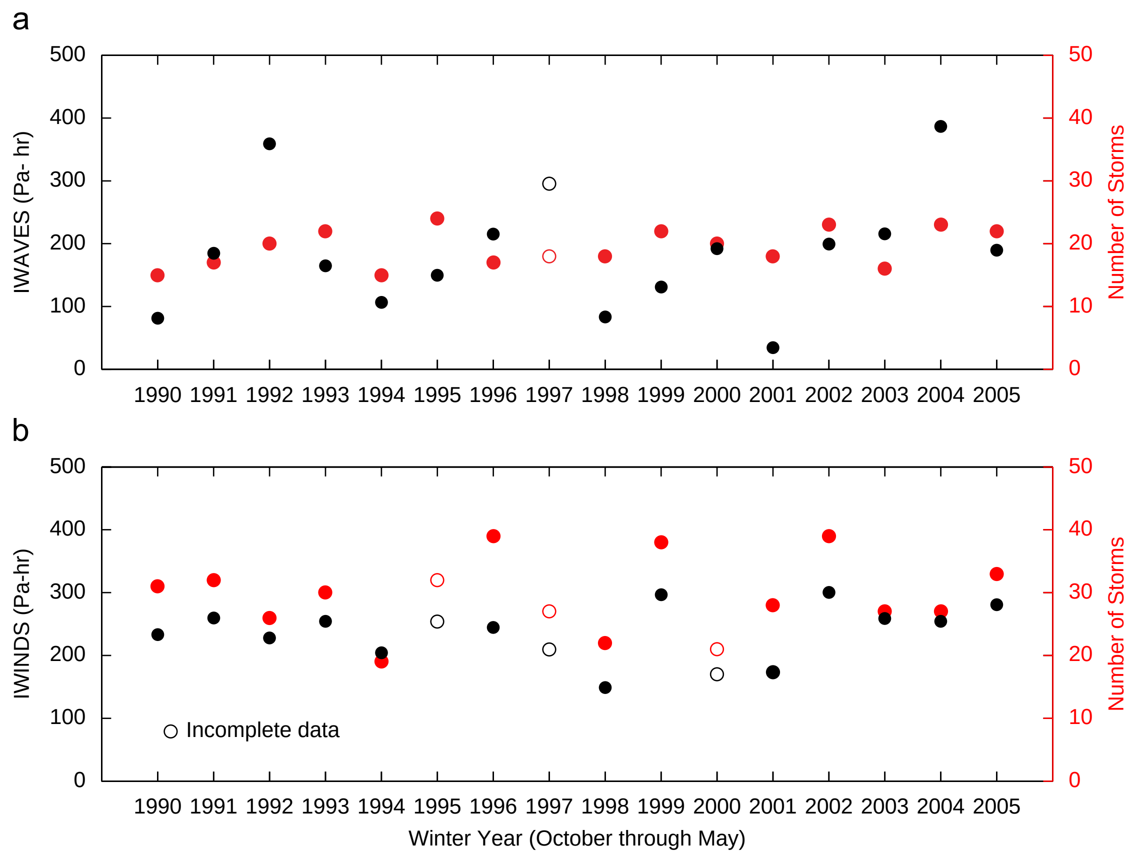

Fig. 9. Sum of IWAVE (a) and IWINDS (b) for all storms between 1 October and 31 May of the following year (an integrated measure of the storm activity for each winter season), and the number of storms in the same time interval. The winter season of 1995 is missing wind observations from 1 April 1996 to 22 April 1996, 1997 is missing wave and wind observations from 1 October to 11 November 1997, and the winter season of 2000 is missing wind data from 1 January to 31 March 2001; the true values for these years (open symbols) are most likely higher than those shown.

Table 4
IWAVES and IWINDS summed over the period 1 October– 31 May of the following year (see Fig. 9)

Start year	No. of IWAVES storms	Total IWAVES (Pa h)	Average IWAVES per storm (Pa h)	No. of IWINDS storms	Total IWINDS (Pa h)	Average IWINDS per storm (Pa h)
1990	15	81	5.4	31	233	7.5
1991	17	185	10.9	32	259	8.1
1992	20	359	17.9	26	228	8.8
1993	22	165	7.5	30	254	8.5
1994	15	107	7.1	19	204	10.8
1995	24	150	6.2	32	254	7.9
1996	17	215	12.7	39	245	6.3
1997	18	296	16.4	27	210	7.8
1998	18	83	4.6	22	149	6.8
1999	22	131	5.9	38	297	7.8
2000	20	192	9.6	21	170	8.1
2001	18	34	1.9	28	173	6.2
2002	23	200	8.7	39	300	7.7
2003	16	216	13.5	27	259	9.6
2004	23	386	16.8	27	254	9.4
2005	22	189	8.6	33	281	8.5

occur as an IWAVES event. The Superstorm of March 1993 ranked 29th and 47th by IWINDS and IWAVES, respectively, but ranked 3rd based on departures from climatology over the period 1948–2000 (Hart and Grumm, 2001).

May 2005 was unique with respect to the strength and number of northeast storms. The storms on May 7 and 22 were ranked 24th and 9th, respectively, by IWINDS, and 24th and 14th, respectively, by IWAVES; if added together, these storms become the second strongest event ranked by IWINDS (exceeding the 28 October 1991 storm) and the fifth strongest event ranked by IWAVES. May 2005 was the only month and year in which 2 of the 9 northeast storms were among the strongest 25 defined by IWINDS; these were the only storms of the 9 strongest northeast storms to occur in the spring. In addition, May 2005 was the only month in the 17-year record that two of the nine strongest northeast storms ranked by IWINDS occurred in the same month and year.

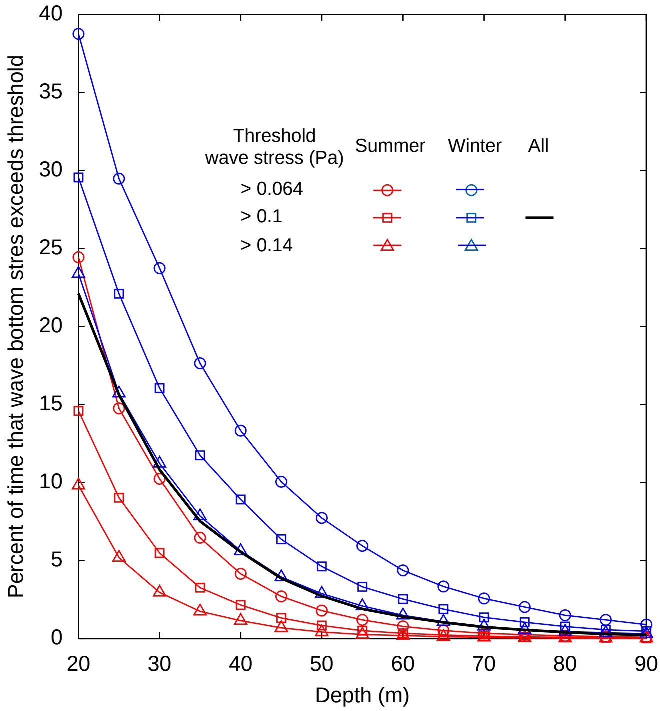

Fig. 10. Percentage of time that wave bottom stress caused by surface waves exceeded 0.064, 0.1, and 0.14 Pa as a function of water depth and season. The bottom stress was calculated at 5 m intervals (symbols) for winter (October–May) and summer (June–September) from significant wave height and dominant wave period observations at NDBC Buoy 44013 for the period 1990–2006. At a water depth of 50 m, bottom-wave stress exceeded 0.1 Pa about 5% of the time in winter and about 1% of the time in summer.

IWAVES integrated over the winter season (October–May), a measure of interannual variability, ranged by about a factor of 11; the winters during which the IWAVES sum was largest were 1992–1993 and 2004–2005 and the sum was smallest in 2001–2002 (Figs. 5 and 9, Table 4). The sum of IWAVES (range 34–386 Pa h) was more variable than the sum of IWINDS (149–300 Pa h) during the winters. In some years individual storms contributed most to the winter sum (for example, the IWAVES for the October 1991 storm contributed 63% to the IWAVES sum for the 1991–1992 winter); in some years storms in winter dominated the sum (for example, January–March 1998 to the 1997–1998 winter); and in some cases events in fall, winter, and spring were all significant contributors (for example, the 2004–2005 winter season) (Fig. 5). The IWAVES for the December 1992 storm (individually ranked 1) contributed about 44% to the sum for the 1992–1993 winter, and the IWAVES for the January and May 2005 storms (individually ranked 6th, 14th, and 24th) contributed about 38% to the sum for the 2004–2005 winter.

The December 1992 northeaster was the strongest based on IWAVES and caused the largest changes in surficial sediment texture and contaminant concentrations at site 3 (Fig. 1) in western Massachusetts Bay (Bothner et al., 2007). Similar textural changes were not observed for the second and third-ranked northeasters of October 1991 and December 2003. One explanation for the difference in sediment response among these strong storms is that the direction of the vector-averaged wind stress for the December 1992 storm was from 54°, whereas the direction for the other two storms was from 24° and 9°, respectively. Numerical simulations suggest that the wind stress associated with the December 1992 storm caused transport from the area offshore of Boston Harbor toward site 3, whereas the transport associated with the wind stress more from the north was southeastward in a relatively narrow band along the coast (Figs. 14 and 15 in Warner et al., 2008). A more detailed modeling simulation of these three largest storms is needed to investigate the possible reasons for the different degree of sediment deposition at site 3. In addition to wind direction, the sequence and spacing of storms and the timing with respect to season and other environmental factors may influence changes on the sea floor caused by IWAVES events of similar magnitude.

A number of investigations have been carried out to understand the effect of storms on sediment transport on a wide range of continental shelves. For example, recent experiments on the northern California shelf (Guerra et al., 2006; Ogston et al., 2004) and in the Adriatic (Fain et al., 2007) collected long-term (5 and 3 years duration, respectively) near-bottom wave, current and suspended-sediment observations to investigate sediment resuspension, transport, and interannual variability. These studies focused on the direction and magnitude of sediment transport, calculated as the product of suspended sediment concentration and velocity, and on the percent of time that bottom wave-orbital velocities exceeded a threshold on a seasonal and yearly basis; they did not rank individual storm events. The studies show that bottom-wave stress is the major process responsible for resuspending sediments in these regions, and that storms occur in a winter season. The percent exceedance of the oscillatory wave current above a threshold varied by a factor of 2–3 in these locations over the years measured. The larger interannual change (factor of 11) observed in the Massachusetts Bay IWAVES metric may be due to the longer 17-year record and because IWAVES incorporates both the duration and magnitude of the storm events that are not reflected in percent exceedance.

Time-series of measurements of significant wave height and period were initiated in the United States in the mid-1970s. Thus calculations of IWAVES and IWINDS could be carried out for other coastal regions, but will be limited to the last 30 years. A climatological study over a longer time span might utilize waves hindcast from models, as done by Dolan and Davis (1992), but this would require a model domain sufficient to include waves generated in distant regions that affect the area of interest. Wave hindcasts would be more accurate for semi-enclosed areas, such as Boston Harbor or Cape Cod Bay, where locally generated waves are the dominant contributor to the wave field.

7. Summary

Storms, particularly northeasters, strongly influence the weather in New England. In addition to the effects caused by the surface wind stress, the sea floor is affected by the bottom stress caused by these storms. This paper uses the wave bottom stress integrated over the duration of a storm as a metric for storm effects on the sea floor. The metric, called IWAVES, combines storm duration and magnitude of bottom stress and is similar to the measure of storm power based on surface waves defined by Dolan and Davis (1992). A different metric based on bottom stress, for example the maximum stress, might be more appropriate than the integrated stress for some processes. Bottom stress was calculated by using near-bottom wave-orbital velocities calculated from surface observations of significant wave height and dominant wave period by the methods outlined in Wiberg and Sherwood (in press).

The integrated bottom stress, called IWAVES, is used to identify, characterize, and rank storms on the basis of surface-wave observations in Massachusetts Bay. The largest storm occurred in December 1992 (the Blizzard of 1992); the next largest storms occurred in October 1991 (the Perfect Storm), December 2003, and March 2001. These storms were all northeasters. The winters (October–May) with the largest IWAVES activity were 1992–1993 and 2004–2005 and the winter with the smallest was 2001–2002. May 2005 was the only month and year in which 2 of the 9 northeast storms were among the strongest 25 defined by IWINDS; these 2 were also the only storms of the 9 strongest northeast storms to occur in the spring.

The IWAVES storm metric identifies events with the potential to affect the sea floor through surface-wave-generated bottom stress. The new metric incorporates both the storm duration and stress magnitude. The goal of identifying and ranking storms using the IWAVES metric is to facilitate understanding of the effects of large storms on the sea floor.

Acknowledgments

We thank R.P. Signell, J.C. Warner, and two anonymous reviewers for helpful comments on the manuscript. This work was supported by the US Geological Survey Coastal and Marine Geology Program.

References

Anderson, D.M., Keafer, B.A., Geyer, W.R., Signell, R.P., Loder, T.C., 2005a. Toxic *Alexandrium* blooms in the western Gulf of Maine: the plume advection hypothesis revisited. Limnology and Oceanography 50 (1), 328–345.

Anderson, D.M., Keafer, B.A., McGillicuddy Jr., D.J., Mickelson, M.J., Keay, K.E., Libby, P.S., Manning, J.P., Mayo, C.A., Whittaker, D.K., Hickey, J.M., He, R., Lynch, D.R., Smith, K.W., 2005b. Initial observations of the 2005 *Alexandrium fundyense* bloom in southern New England: general patterns and mechanisms. Deep-Sea Research II (52), 2856–2867.

Bothner, M.H., Butman, B., 2007. Introduction, geologic setting, and program overview. Section. 1. In: Bothner, M.A., Butman, B. (Eds.), Processes Influencing the Transport and Fate of Contaminated Sediments in the Coastal Ocean—Boston Harbor and Massachusetts Bay. US Geological Survey Circular 1302, pp. 2–11. Also online at: 〈http://pubs.usgs.gov/circ/2007/1302〉.

Bothner, M.H., Casso, M.A., Lamothe, P.J., Baldwin, S.M., Rendigs, R.R., 2007. Using sediments to monitor environmental change in Massachusetts Bay and Boston Harbor. Section 7. In: Bothner, M.A., Butman, B. (Eds.), Processes Influencing the Transport and Fate of Contaminated Sediments in the Coastal Ocean—Boston Harbor and Massachusetts Bay. US Geological Survey Circular 1302, pp. 48–55. Also online at: 〈http://pubs.usgs.gov/circ/2007/1302〉.

Butman, B., Bothner, M.H., Alexander, P.S., Lightsom, F.L., Martini, M.A., Gutierrez, B.T., Strahle, W.S., 2004. Long-term Observations in Western Massachusetts Bay Offshore of Boston, Massachusetts: Data Report for 1989–2002. USGS Digital Data Series DDS-74, Version 2, DVD-ROM. Also online at: 〈http://pubs.usgs.gov/dds/dds74/〉.

Butman, B., Alexander, P.S., Scotti, A., Beardsley, R.C., Anderson, S.P., 2006. Large internal waves in Massachusetts Bay transport sediments offshore. Continental Shelf Research 26 (17/18), 2029–2049.

Butman, B., Warner, J.C., Bothner, M.H., Alexander, P.S., 2007. Predicting the transport and fate of sediments caused by northeast storms. Section 6. In: Bothner, M.A., Butman, B. (Eds.), Processes Influencing the Transport and Fate of Contaminated Sediments in the Coastal Ocean—Boston Harbor and Massachusetts Bay. US Geological Survey Circular 1302, pp. 38–47. Also online at: 〈http://pubs.usgs.gov/circ/2007/1302〉.

Dolan, R., Davis, R.E., 1992. An intensity scale of Atlantic coast northeast storms. Journal of Coastal Research 8 (4), 840–853.

Fain, A., Ogston, A., Sternberg, R.W., 2007. Sediment transport event analysis on the western Adriatic continental shelf. Continental Shelf Research 27, 431–451.

Guerra, J.V., Ogston, A.S., Sternberg, R.W., 2006. Winter variability of physical processes and sediment-transport events on the Eel River shelf, northern California. Continental Shelf Research 26 (17/18), 2050–2072.

Hart, R.E., Grumm, R.H., 2001. Using normalized climatological anomalies to rank synoptic-scale events objectively. Monthly Weather Review 129 (9), 2426–2442.

Junger, S., 1997. The Perfect Storm: A True Story of Men Against the Sea. W.W. Norton, New York, NY, 227pp.

Kalnejais, L.J., Martin, W.R., Signell, R.P., Bothner, M.H., 2007. The role of sediment resuspension in the remobilization of particulate-phase metals from coastal sediments. Environmental Science and Technology 41(7), 2282–2288, DOI:10.1021/es061770z.

Large, W.G., Pond, S., 1981. Open momentum ocean flux measurements in moderate to strong winds. Journal of Physical Oceanography 11, 324–336.

Madsen, O.S., 1994. Spectral wave-current bottom boundary layer flows. In: Proceedings, 24th International Conference on Coastal Engineering, American Society of Civil Engineers, Kobe, pp. 384–398.

National Oceanic and Atmospheric Administration National Weather Service, 2001. Daily Weather Maps, Weekly Series, March 05–March 11, 2001. NOAA Climate Prediction Center, Washington, DC, 8pp. Also online at: 〈http://docs.lib.noaa.gov/rescue/dwm/data_rescue_daily_weather_maps.html〉.

National Oceanic and Atmospheric Administration National Data Buoy Center, Historical Data, online at: 〈http://www.ndbc.noaa.gov/historical_data.shtml〉.

Ogston, A.S., Guerra, J.V., Sternberg, R.W., 2004. Interannual variability of nearbed sediment flux on the Eel River Shelf, northern California. Continental Shelf Research 24 (1), 117–136.

Roworth, E.T., Signell, R.P., 1998. Construction of digital bathymetry for the Gulf of Maine. US Geological Survey Open-File Report 98–801. Online at: 〈http://pubs.usgs.gov/of/1998of98-801/index.htm〉.

Soulsby, R.L., 1987. Calculating bottom orbital velocity beneath waves. Coastal Engineering 11, 371–380.

Warner, J.C., Butman, B., Dalyander, P.S., 2008. Storm-driven sediment transport in Massachusetts Bay. Continental Shelf Research 28 (2), 257–282.

White, S.J., 1970. Plane thresholds of fine-grained sediments. Nature, London 228, 152–153.

Wiberg, P.L., Sherwood, C.R. Calculating wave-generated bottom orbital velocities from surface wave parameters. Computers in Geosciences, in press.

Wiberg, P.L., Drake, D.E., Harris, C.K., Noble, M., 2002. Sediment transport on the Palos Verdes shelf over seasonal to decadal time scales. Continental Shelf Research 22, 987–1004.

Zhang, K.Q., Douglas, B.C., Leatherman, S.P., 2000. Twentieth-century storm activity along the US east coast. Journal of Climate 13 (10), 1748–1761.

Zielinski, G.A., 2002. A classification scheme for winter storms in the eastern and central United States with an emphasis on nor'easters. Bulletin of the American Meteorological Society 83 (1), 37–51.